

Wind tunnel study of the flow field around the blade of a HAWT

Takao Maeda, Yasunari Kamada, Yusaku Sakai, Naoki Takahara
Department of Mechanical Engineering, Mie University
1515 Kamihama-cho, Tsu, Mie 514-8507, Japan
Phone:+81-59-231-9382 /Fax:+81-59-231-1572 /E-mail:maeda@mach.mie-u.ac.jp

Summary

The objective of this study is the investigation of the flow field around a 2.4m-diameter three-bladed upwind horizontal axis wind turbine. The flow field around the rotor blade was measured with the use of Laser Doppler Velocimetry Method (LDV). The angle of attack is calculated from the flow vectors. The flow field in the near wake shows strong fluctuations at stall condition. The circulation around the blade sections, as a quantitative parameter to study the rotor performance, is also calculated by flow vectors around rotor blade. The velocity vectors at optimum tip speed ratio operation show a smooth flow around the blade and the bound vortex around blade cross-section seems to be persistent. On the other hand, the velocity vectors at stall condition demonstrate significant fluctuations in the near wake and separation on the blade suction surface was observed. The circulation along blade spanwise section was calculated at the certain control volume. By the observation of flow field and calculated results of circulation, it seems that the flow is separated at the blade from middle-span region to tip region at stall condition. No separation was observed at the blade root region. The turbulence intensity and vorticity of the flow in the near wake at stall condition was also higher than those at optimum operation. The angle of attack, calculated by flow vector upstream the blade, has a decreasing trend with increasing the distances from blade leading edge. For the middle-span to tip region, the angle of attack at -30 degrees azimuth angle upstream rotor blade agrees well with that for the design angle of attack for BEM calculation.

Keywords: Wind turbine, Velocity, Laser Doppler Velocimetry, Circulation, Angle of attack, Separation

1. Introduction

Many of the aerodynamic phenomena contributing to the observed effects on wind turbines are now known, but the details of the flow are still poorly understood and are challenging to predict accurately. Horizontal axis wind turbines frequently experience unexpectedly high aerodynamic loads during service. Though in recent years there has been substantial progress in the aerodynamic modeling and design of horizontal axis wind turbine, there is still a failure to predict high aerodynamic loads.

Mie University in Japan has been actively engaged and contributed to the rotor aerodynamic research. The most significant approach was the participation in the IEA Annex XVIII, and the pressure measurement on the rotor blade was carried out at the task. The efforts have been persistent to investigate in detail the flow field around the rotor.

This paper describes the measurement of the flow field around rotor blade. Three-bladed upwind rotor is tested in a wind tunnel. The rotor has a diameter of 2.4 m. Flow field around rotor blade is measured with the use of two-dimensional LDV. The local angle of attack upstream of blade leading edge was calculated from the flow vectors. The circulation around the blade sections was also calculated by flow vectors around the rotor blade. Relationship between

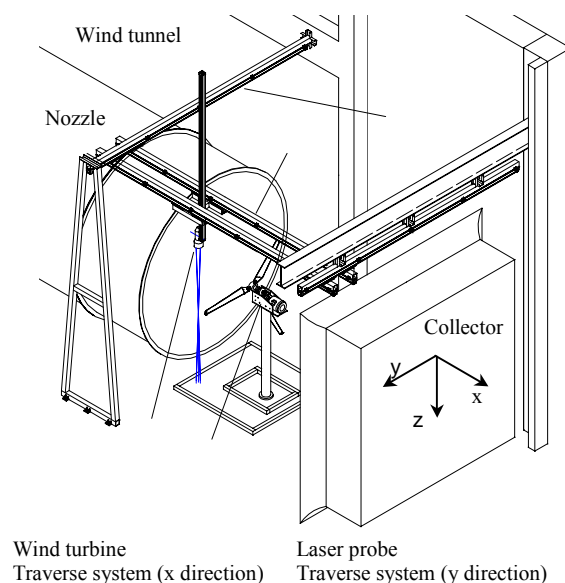


Fig.1 Experimental apparatus

the rotor performance and the flow behavior is discussed.

2. Measurement Setup and Procedure

The experiments were carried out in an open test section of Goettingen wind tunnel with an outlet diameter of 3.6m and maximum wind speed of 30m/s as shown in Fig.1. The test wind turbine was three-bladed horizontal axis wind turbine which has a diameter of 2.4m. The rotor plane was set at 1D downstream of wind tunnel outlet. The rotor was rotated in counter-clockwise direction viewed from upwind. The blade sections are composed by DU and NACA airfoils through blade root to tip. The chord lengths of the blade tip is 85 mm and the blade is twisted 18.3 degrees through blade root to tip. It is equipped with a torque meter, a variable speed generator for controlling the rotor speed, a photocell for measuring azimuth angle, and a rotational speed sensor in the nacelle.

Figure 2 shows the fixed coordinate system used for the velocity measurements. The time dependent flow field around the blade was investigated by means of two-dimensional Laser Doppler Velocimetry (LDV) methods. The optical head was mounted on three-dimensional traversing mechanism. Changing the direction of the probe, the velocity components u , v on the x - y plane and u , w on the x - z plane were measured. Therefore, a three dimensional velocity field around the rotating blade was composed. The optical head was equipped with a beam-expander to increase the focal length up to 2000 mm. The power of the Argon laser source was 4 W. The wavelength of the blue color and green color beams were 488.0 nm and 514.5 nm, respectively. The LDV was operated in a backscatter mode close to the blade surface. The flow was seeded with mixture of oil and water resulting in 1 μ m-diameter particles. The control volume of LDV was 0.15mm in diameter and 4.3mm in length. The initiation and synchronization of the data were realized by means of a photocell. Measurements were phase-averaged around 9 rotations of the rotor. The azimuth angle of blade top position was defined as 0 degree. The LDV measurement was carried out every 0.4 degree in the region of azimuth angle of 60 to 180 degrees. In this paper, the results of 7m/s of the undisturbed flow velocity are shown.

3. Results and Discussion

3.1 Power Coefficient of Rotor

Figure 3 shows the power coefficient curve of the test wind turbine. The measurement was carried out at a blade pitch angle of -2 degrees. The maximum power coefficient reaches the value of 0.434 at optimum tip speed ratio of $\lambda = 4.95$. Since the wind tunnel measurement was done at constant wind speed condition, the torque is decreasing with decreasing rotor speed, so that there is a stall state at lower tip speed ratio than optimum one. The power coefficient is achieved at $C_p=0.202$ for the tip speed ratio of $\lambda = 3.72$ at certain stall state. When the rotor speed was increased over the optimum operation, overrunning state was observed at higher tip speed ratio. For the tip speed ratio of $\lambda = 6.50$, the power coefficient at this overrunning state was $C_p=0.335$.

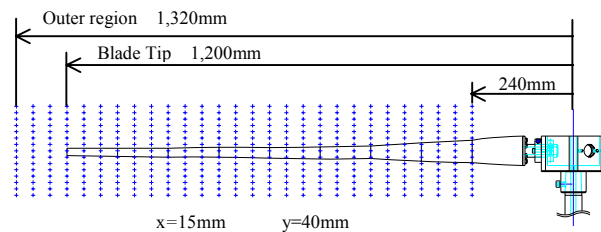


Fig.2 Measurement positions

3.2 Velocity Field around Rotor

Figure 4 shows the velocity vectors around the blade at the $r/R=0.7$ spanwise section. For the velocity vectors for the optimum tip speed ratio condition of $\lambda = 4.95$, it seems that the flow is attached along the blade surface and a bound vortex appears around measurement section. For the velocity vectors for stalling condition of $\lambda = 3.72$, the flow is separated on the suction surface and the separated vortex is observed behind the trailing edge. It is also observed

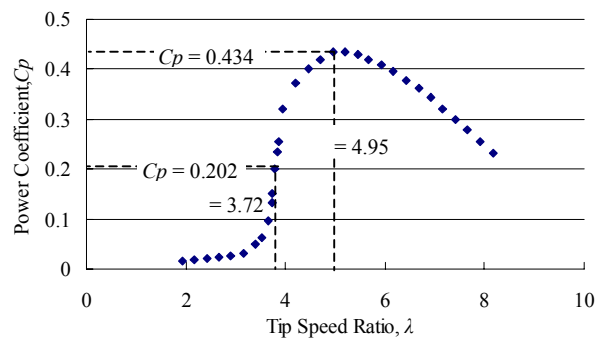


Fig.3 Power curve

the disturbed flow field until far away downwind of the blade.

3.3 Circulation calculated by Velocity Vectors

The effect on section performance due to velocity field is obtained by calculation of circulation. Figure 5 shows the control volume of calculation of section circulation. The control volume for calculation of circulation is depending on the radius in this study. Considering the circulation area as a summation of the elementary areas having at nodes the measuring points, as shown in Fig.6, the integral over the closed peripheral rectangular path gives the circulation strength, Γ , at a certain radial section. The circulation Γ is non-dimensionalized by the $U_0 R$ for considering the effect of the differences of radius.

Figure 7 shows the non-dimensional circulation distribution around the blade section at $r/R=0.7$ against azimuth angle. For the optimum tip speed ratio condition, the non-dimensional circulation is increasing with the blade approaching to the control volume. The non-dimensional circulation is suddenly decreased at the blade passing the control volume of azimuth angle of 90 degrees. After the blade passing the control volume, the value of circulation becomes almost zero. For the stalling condition, the value of non-dimensional circulation is smaller than those for the optimum tip speed ratio condition. After the blade passing the control volume, the counter-vortex against the bound vortex is appeared behind the trailing edge. The vortex is observed from the range of azimuth angle of 100 degrees until 130 degrees. These vortices seem to become the drag for the blade.

Figure 8 shows the spanwise non-dimensional circulation distribution around the blade for the optimum tip speed ratio condition of $\lambda = 4.95$ and stalling condition of $\lambda = 3.72$. The circulation is held from the blade root to the tip for the optimum tip speed ratio condition. For the stalling condition, the value of circulation is much lower in the region of $0.5 < r/R < 1.0$ than those for the optimum condition. It seems that the stall is occurred at $r/R > 0.5$ and the lift arises on the blade becomes low. The distribution of circulation is much varied at $r/R > 0.5$ because the vortex due to separation is passed through control volume. On the other hand, the circulation has a large value for the inner region at $0.2 < r/R < 0.4$, so that the thick airfoil shows suitable characteristics for the blade root aerodynamics.

3.4 Angle of Attack measured by Flow Velocity

It is difficult to determine the angle of attack for the rotating blade. In this paper, the angle of attack is tried to determine by the velocity vectors measured by LDV. Figure 9 shows comparison of the distribution of angle of attack calculated by BEM and measured by LDV. The angle of attack by BEM is the design value for the blade and is calculated every

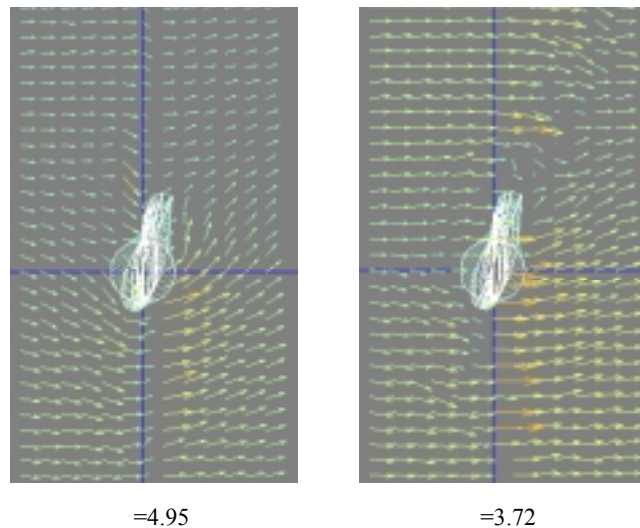


Fig.4 Velocity distribution ($r/R = 0.7$)

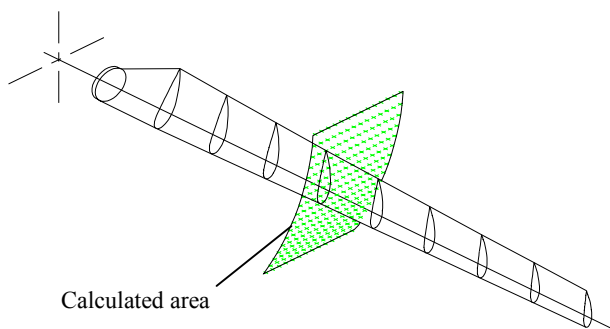


Fig.5 Calculated area of circulation

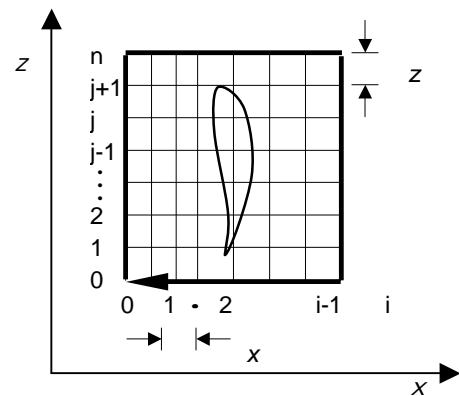


Fig.6 Definition of calculation of circulation

$r/R=0.1$ interval. The measured angle of attack by LDV is determined by the flow angle in the rotor plane at azimuth angle around 60 degrees (equal to -30 degrees upstream of the blade) where the pressure distributions of two-dimensional and rotating situation are almost identified. The angle of attack of BEM agrees well with the measured value at $r/R=0.7$ and 0.85. However, the angle of attack calculated by BEM shows much differences from those for measured one at $r/R=0.3$. It should be considered for the determination of the angle of attack near the blade root by the effects of the hub and nacelle on the flow and also complex flow effects on the root region.

4. Conclusion

The flow field around a rotating blade of a three-bladed upwind turbine in the wind tunnel is investigated. The comparison of the results for optimum operation and stall condition is shown. Velocity data were collected by the use of Laser Doppler Velocimetry method. Main results of this study is obtained as follows:

1. For the stalling operation, the disturbed flow area in the wake is larger than compared to optimum operational conditions. A remarkable stall is observed near the blade tip in case of small tip speed ratios. No stall is found near the blade root. Flow seems to be separated from middle-span region to the tip.
2. Spanwise distribution of the circulation strength around the blade shows that larger circulation was found to be in case of stalling condition near the blade root. The distribution of the circulation varies at the outer region of the blade for the stalling condition.

References

1. W.A. Timmer, R.P.J.O.M. van Rooy, Wind tunnel results for a 25% thick wind turbine blade aerofoil Proc. Euro. Union Wind Energy Conf. 93, Lubeck-Travemunde, Germany, 1993; 416-419
2. P.R.Ebert, D.H.Wood, The near wake of a model horizontal-axis wind turbine at runaway, Renewable Energy, 25, 2002; 41-54.
3. N.J Vermeer, G.J.W. van Bussel, Velocity measurements in the near wake of a model rotor and comparison with theoretical results, Proc. Euro. Wind Energy Conf. 90, Madrid, Spain, 1990; 218-222.

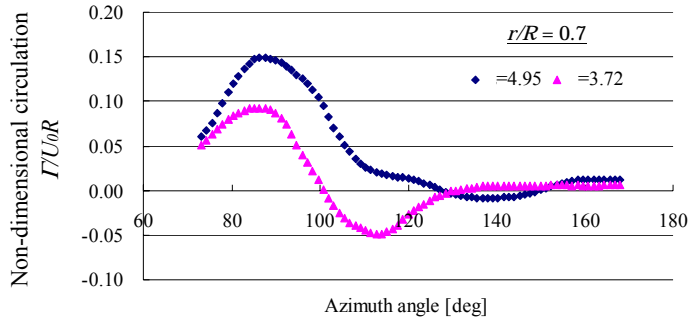


Fig.7 Fluctuation of circulation at $r/R=0.7$

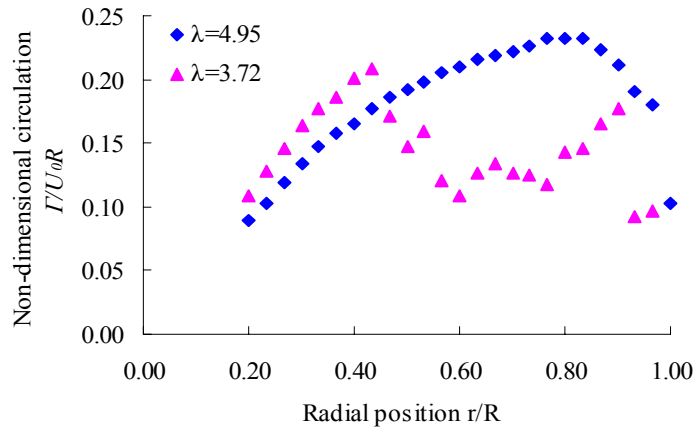


Fig. 8 Spanwise distribution of circulation

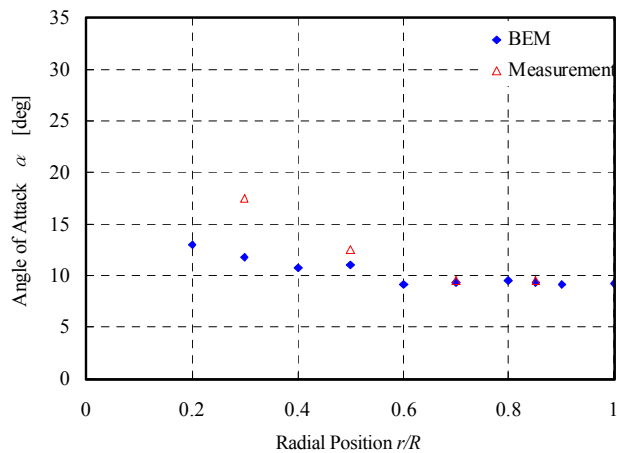


Fig. 9 Spanwise distribution of angle of attack